Efficient Modelling Methodology for Reconfigurable Underwater Robots

Nielsen, Mikkel Cornelius; Blanke, Mogens; Schjølberg, Ingrid

Published in:
IFAC-PapersOnLine

Link to article, DOI:
10.1016/j.ifacol.2016.10.324

Publication date:
2016

Document Version
Peer reviewed version

Efficient Modelling Methodology for Reconfigurable Underwater Robots

Mikkel Cornelius Nielsen [*,**] **Mogens Blanke** [*,**]
Ingrid Schjølberg [*]

[*] *Centre for Autonomous Marine Operations and Systems, Department of Engineering Cybernetics, Norwegian University of Science and Technology, Trondheim, Norway*
[**] *Department of Electrical Engineering, Technical University of Denmark, Lyngby, Denmark*

Abstract: This paper considers the challenge of applying reconfigurable robots in an underwater environment. The main result presented is the development of a model for a system comprised of N, possibly heterogeneous, robots dynamically connected to each other and moving with 6 Degrees of Freedom (DOF). This paper presents an application of the Udwadia-Kalaba Equation for modelling the Reconfigurable Underwater Robots. The constraints developed to enforce the rigid connection between robots in the system is derived through restrictions on relative distances and orientations. To avoid singularities in the orientation and, thereby, allow the robots to undertake any relative configuration the attitude is represented in Euler parameters.

Keywords: Udwadia-Kalaba, Multi-body Dynamics, Quaternion, Autonomous Underwater Vehicles, Reconfigurable Robots

1. INTRODUCTION

The offshore industry is becoming technologically ever more demanding and visions foresee production facilities will move from the ocean surface to the seabed. Consequently, robotic solutions will have to solve increasingly diverse tasks and collaborating and reconfigurable robots are envisaged to become important in support of this technology evolution. This paper deals with modelling for control of multi-robot systems with an aim of being able to automate the modelling of vehicles that should be able to connect or disconnect and form configurations required for a specific task. The modelling should be able to be done without human intervention other that the definition of dynamics for the individual vehicle.

Present solutions focus on Remotely Operated Vehicles (ROVs) for power demanding tasks such as positioning of subsea modules during the installation phase Henriksen et al. (2015). Several low-power tasks are, however, better carried out by non-tethered vehicles, and in the long term a modular reconfigurable multi-robot solution can provide high control authority and flexibility. This means that several autonomous vehicles work together to perform a joint task. Multi-vehicle systems for underwater applications were studied in Belleter and Pettersen (2014, 2015) where formation control was the main objective. The focus in this paper is modular reconfigurable multi-robot system that is capable of physically changing its morphology. From a reconfiguration point-of-view work has mainly focused on modularity in the physical sense. An underwater platform with docking capability to offload data between a sensor network and an Autonomous Underwater Vehicle (AUV) was presented in Vasilescu et al. (2005), and Mintchev et al. (2012, 2014) presented a system of anguilliform AUVs with the ability of docking to each other, utilising passive magnets to align the vehicles for docking. The system resulting from physically coupling and de-coupling of the vehicles is a multi-body system with dynamic topology. The modular robotics community predominantly focus on Fuzzy Logic control of multi-body systems, but when high precision control is needed, modelling is a necessary prerequisite. Generic modelling for individual underwater vehicles has been extensively treated in Antonelli (2014) and Fossen (2011), so the challenge for a multi-body cluster is to be able to describe the nonlinear dynamics of the cluster from the dynamics of individual members.
The objective of the present effort is hence to provide a modelling tool that can describe the dynamic properties of a morphology from the geometry of the cluster and properties of its' members. The challenge with traditional modelling methods is the difficulties that arise from constraints when robots connect. The paper develops the equations of motion for a system comprised of N rigidly connected robots based on the Udwadia-Kalaba Formulation (Udwadia and Schutte, 2012). We exploit this framework using quasi-velocities to derive the constraints imposed by rigid connections, using a quaternion formulation to avoid singularities. The contribution of the paper is to show how the Udwadia-Kalaba methodology can be applied to reconfigurable underwater robots, and in particular can deal with redundant constraints in a robust manner. The contribution of the paper is to show how automatic generation of models is possible for reconfigurable underwater

[1] This work was supported by the Research Council of Norway through the Centres of Excellence funding scheme, the AMOS project, grant number 223254.

systems.

The paper first lists the notation along with the kinematics and kinetics needed. Section 3 discusses the general problem of constrained dynamics and Section 4 shown how the Udwadia-Kalaba approach can be applied to handle the constraints of a generic morphology of connected underwater robots. Finally, a series of simulations verify the automated modelling concept, and Section 7 provides conclusions and perspectives.

2. RIGID-BODY MODEL

2.1 Notation and Kinematics

This section summarises the notation broadly used in the area of underwater vehicles, as this was introduced in Fossen (2011). For the purpose of this paper the earth-fixed North-East-Down (NED) frame, denoted $\{n\}$, will be assumed inertial. The frame configuration variables denoted $\boldsymbol{\eta} = [\boldsymbol{p}^n_{b/n}, \boldsymbol{u}]^T \in \mathbb{R}^7$ comprise of the position $\boldsymbol{p}^n_{b/n} = [x^n, y^n, z^n]^T$ and the attitude represented as a unit quaternion to avoid singularities $\boldsymbol{u} = [\eta, \varepsilon_1, \varepsilon_2, \varepsilon_3]^T$. Attached to each body in the system is a local body-fixed frame denoted $\{b\}$. The body-fixed velocities denoted $\boldsymbol{\nu}$ as

$$\boldsymbol{\nu} = [u \ v \ w \ p \ q \ r]^T \in \mathbb{R}^6 \tag{1}$$

As with the configuration vector the body-fixed velocity vector can be separated into linear velocities $\boldsymbol{\nu}_1 = [u, v, w]^T$ and angular velocities $\boldsymbol{\nu}_2 = [p, q, r]^T$. To relate the NED and body-fixed frame the rotation matrix $\boldsymbol{R}^n_b$ defined below

$$\boldsymbol{R}^n_b = \begin{bmatrix} 1-2\left(\varepsilon_2^2+\varepsilon_3^2\right) & 2\left(\varepsilon_1\varepsilon_2-\varepsilon_3\eta\right) & 2\left(\varepsilon_1\varepsilon_3+\varepsilon_2\eta\right) \\ 2\left(\varepsilon_1\varepsilon_2+\varepsilon_3\eta\right) & 1-2\left(\varepsilon_1^2+\varepsilon_3^2\right) & 2\left(\varepsilon_2\varepsilon_3-\varepsilon_1\eta\right) \\ 2\left(\varepsilon_1\varepsilon_3-\varepsilon_2\eta\right) & 2\left(\varepsilon_2\varepsilon_3+\varepsilon_1\eta\right) & 1-2\left(\varepsilon_1^2+\varepsilon_2^2\right) \end{bmatrix} \tag{2}$$

To relate the attitude change in the inertial frame $\{n\}$ with the angular velocities $\boldsymbol{\omega}^b_{b/n}$ around the principle axes of the body-fixed frame $\{b\}$ the angular transformation matrix $\boldsymbol{T}_u$ is used.

$$\dot{\boldsymbol{u}} = \boldsymbol{T}_u \boldsymbol{\omega}^b_{b/n} \tag{3}$$

where $\boldsymbol{T}_u$ is defined as

$$\boldsymbol{T}_u = \frac{1}{2}\boldsymbol{H}^T = \frac{1}{2}\begin{bmatrix} -\varepsilon_1 & -\varepsilon_2 & -\varepsilon_3 \\ \eta & -\varepsilon_3 & \varepsilon_2 \\ \varepsilon_3 & \eta & -\varepsilon_1 \\ -\varepsilon_2 & \varepsilon_1 & \eta \end{bmatrix} \tag{4}$$

such that $\boldsymbol{H}$ is

$$\boldsymbol{H} = [-\boldsymbol{\varepsilon} \ \eta\boldsymbol{I}_3 - \boldsymbol{S}(\boldsymbol{\varepsilon})] \in \mathbb{R}^{3\times 4} \tag{5}$$

where $\boldsymbol{S}(\boldsymbol{\varepsilon})$ is the skew-symmetric matrix such that $\boldsymbol{S}(\boldsymbol{\lambda})^T = -\boldsymbol{S}(\boldsymbol{\lambda})$ and it is defined as

$$\boldsymbol{S}(\boldsymbol{\lambda}) = \begin{bmatrix} 0 & -\lambda_3 & \lambda_2 \\ \lambda_3 & 0 & -\lambda_1 \\ -\lambda_2 & \lambda_1 & 0 \end{bmatrix} \tag{6}$$

To account for the environmental disturbances the model will be formulated in relative velocity $\boldsymbol{\nu}_r$.

$$\boldsymbol{\nu}_r = \boldsymbol{\nu} - \boldsymbol{\nu}_c \tag{7}$$

where $\boldsymbol{\nu}_c$ is the velocity of the water current in the body-fixed frame.

Assumption 1. The current is constant and irrotational in the inertial frame.

Remark 2. Assumption 1 is reasonable in the sense that both amplitude and direction of currents are slowly varying.

Assumption 3. The fluid is viscid, incompressible and irrotational.

Remark 4. Assumption 3 is common in hydrodynamic modelling.

Assumption 5. The cross-flow can be neglected in control applications.

Remark 6. Assumption 5 is not strictly true, however for the purpose of control oriented modelling, the assumption is acceptable.

The kinetic model for marine systems in relative velocity was derived in Fossen (2011) and is shown below

$$\boldsymbol{M}\dot{\boldsymbol{\nu}}_r + \boldsymbol{D}(\boldsymbol{\nu}_r)\boldsymbol{\nu}_r + \boldsymbol{C}(\boldsymbol{\nu}_r)\boldsymbol{\nu}_r + \boldsymbol{g}(\boldsymbol{\eta}) = \boldsymbol{\tau} \tag{8}$$

The model in Eq. (8) form the local model of a combined system. This leads to Section 3, where the general problem of constrained dynamics are presented.

3. CONSTRAINED DYNAMICS

The challenge of constrained dynamics is to ensure physically sound motion of a system where the states are not independent due to imposed constraints. Different approaches exist for solving the constraining forces and thereby the resulting motion of the constrained system. For reconfigurable robots, cyclic configurations can cause redundant constraints to appear and, as a result, the constraint matrix will no longer be full rank. When this occurs, classical modelling methods will fail as they cannot provide a unique solution for the constrained forces. The Udwadia-Kalaba methodology, in contrast, does not require a constraint matrix to be full rank. This section discusses the issues related to modelling of constrained dynamics.

Consider the generalised Newtonian system $\mathcal{G}$

$$\mathcal{G} := \begin{cases} \dot{\boldsymbol{q}} = \boldsymbol{v} \\ \boldsymbol{M}\dot{\boldsymbol{v}} = \boldsymbol{Q} \end{cases} \tag{9}$$

where $\boldsymbol{q} \in \mathbb{R}^{n_q}$ is the vector of generalised coordinates, $\boldsymbol{M} \in \mathbb{R}^{n_q \times n_q}$ is the system inertia matrix and $\boldsymbol{Q} \in \mathbb{R}^{n_q}$ is a vector of generalised forces.

Constraints emerge in such system as a consequence of physical restrictions. A system described by ordinary differential equations (ODE) and with constraints forms a differential-algebraic equation (DAE) system. Such DAE systems are difficult to solve, and are not easily used as basis for control design. The aim of modelling is to get a system description that takes an ODE form.

If constraints appear in *holonomic* form, see definition below, they can be eliminated by coordinate reduction, that, however, results in high complexity descriptions that can be viewed as ODEs on a manifold.

Definition 7. A constraint c is said to be *holonomic* iff it can be represented independently of the generalised velocities $\dot{\boldsymbol{q}}$ such as in the following equation

$$c(\boldsymbol{q}, t) = 0 \tag{10}$$

From a geometric point-of-view the motion of the dynamical system of Eq. (9) would evolve on the sub-manifold $\mathcal{M}$ defined as

$$\mathcal{M} = \{(\boldsymbol{q}, \boldsymbol{v}) : c(\boldsymbol{q}) = 0,\ \nabla_q c(\boldsymbol{q})\boldsymbol{v} = 0\} \tag{11}$$

The motion on the manifold is constrained by $\nabla_q c(\boldsymbol{q})\boldsymbol{v} = 0$ which is often called a *hidden constraint*, since it does not appear explicitly in Eq. (10).

The pose of a rigid body in three dimensional space can be described uniquely by six variables, hence, by six *degrees of freedom*. The holonomic constraint results in a decrease of the degrees of freedom n_f by $n_f = n_q - n_c$, where n_c is the number of constraints and n_q is the number of generalised coordinates.

To illustrate this in a geometric fashion Fig. 1 shows a particle constrained to a manifold by a holonomic constraint, where $\boldsymbol{q} \in \mathbb{R}^3$. The unconstrained motion of the particle would follow the ODE, Eq. (9). The solution for the DAE system requires the information of the constraint to be injected into the ODE part.

One approach to injecting the constraint into the ODEs is by re-parametrisation of the generalised coordinates to obtain a new set of independent coordinates that take the constraint into account. In this case the particles coordinates are $\boldsymbol{q} = [a_1, a_2]$, such that the motion on the sub-manifold c is uniquely defined. The disadvantage of using coordinate reduction is an increase in complexity of the resulting ODEs and the possible difficulty of finding a new set of independent coordinates.

If the constraint is not holonomic or a suitable re-parametrisation cannot be identified, the constraint must be actively enforced. This is done by augmenting the dynamic equation system Eq. (9) with a constraining force $\boldsymbol{Q}_c$ such that

$$\mathcal{G}_c := \begin{cases} \dot{\boldsymbol{q}} = \boldsymbol{v} \\ \boldsymbol{M}\dot{\boldsymbol{v}} = \boldsymbol{Q} + \boldsymbol{Q}_c \end{cases} \tag{12}$$

The difficulty of identifying the constraint force $\boldsymbol{Q}_c$ depends on the differential index of the DAE defined below

Definition 8. (Brenan et al. (1995)). *Differential Index*: The minimum number of times that the constraint of Eq. (10) must be differentiated with respect to the independent variable t to transform the DAE into an ODE.

In Takamatsu and Iwata (2008) the authors state that the difficulty in solving a DAE increases with the Differential Index. Gear and Petzold (1984) suggested that an index reduction is necessary for indices larger than one. Given that a rigid constraint is holonomic, both coordinate reduction and constraint enforcement is possible. However, the modular robotic system under investigation is subject to structural changes during operations. Using coordinate reduction to solve the problem would require a new set of coordinates to be calculated each time a change is introduced in the system. Furthermore, the complexity of the individual robot dynamics can render the model unusable for analytical purposes. Conversely, the constraint enforcement approach is not without flaws. Firstly the

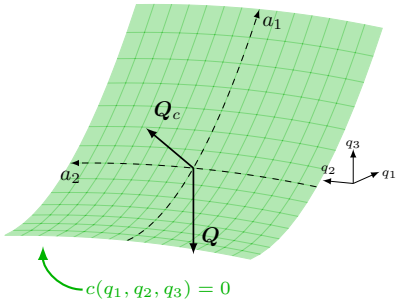

Fig. 1. Motion of a particle constrained to a surface $c(q_1, q_2, q_3) = 0$. There exists an algebraic relationship between the generalised coordinates.

constraint forces required to sustain the solution to the constraint sub-manifold have to be identified. There exists a variety of methods to identify such constraint forces. Bauchau and Laulusa (2008) gave an overview of methods used to enforce constraints in multi-body systems — the most classical approach being Lagrange's multipliers. In Wojtyra and Fraczek (2013) investigated the problem of redundant constraints in relation to multi-body systems and rank deficiency of the resulting constraint matrix.
In a modular robotic system a redundant constraint can appear if a series of connection between different robots leads to a loop-closure. If such a situation occurs, the constraint matrix will become rank deficient and a unique solution may not be possible. The solution is then to manually remove as many redundant constraints until the constraint matrix becomes full rank. In Kalaba and Udwadia (1994) another approach modelling of constrained multi-body dynamics based on Gauss's Principle of Least Constraint was presented. This approach does not require the constraint matrix to be full rank, at the cost of being slightly more computationally heavy. The main feature of this method is the use of a single global equation for modelling, which can be extended to include quasi-velocities.

4. UDWADIA-KALABA EQUATION

In this section, the general Udwadia-Kalaba formulation is presented in quasi-velocities. This is based on the work in Udwadia and Phohomsiri (2007) where the Udwadia-Kalaba formulation was extended to include quasi-velocities and quasi-accelerations. Consider a transformation $\boldsymbol{G}(\boldsymbol{q}) \in \mathbb{R}^{n_s \times n_q}$ such that

$$\boldsymbol{s} = \boldsymbol{G}(\boldsymbol{q})\,\dot{\boldsymbol{q}} \tag{13}$$

where $\boldsymbol{s} \in \mathbb{R}^{n_s}$ is a vector of quasi-velocities and $\boldsymbol{q} \in \mathbb{R}^{n_q}$ and $\dot{\boldsymbol{q}}$ are generalised coordinates and generalised velocities respectively. A general unconstrained Newtonian system can be described in terms of quasi-coordinates as in Eq. (14).

$$\boldsymbol{M}\dot{\boldsymbol{s}}_u = \boldsymbol{S} \tag{14}$$

Where $\boldsymbol{M} \in \mathbb{R}^{n_s \times n_s}$ is the inertia matrix, $\dot{\boldsymbol{s}}_u$ are the unconstrained quasi-accelerations of the system and $\boldsymbol{S} \in \mathbb{R}^{n_s}$ is the generalised forces. In case the system is subjected to constraints the formulation in Eq. (14) can be transformed into the constrained formulation of Eq. (15) by augmenting with an additional constraining force $\boldsymbol{S}_c \in \mathbb{R}^{n_s}$.

$$\boldsymbol{M}\dot{\boldsymbol{s}}_c = \boldsymbol{S} + \boldsymbol{S}_c \tag{15}$$

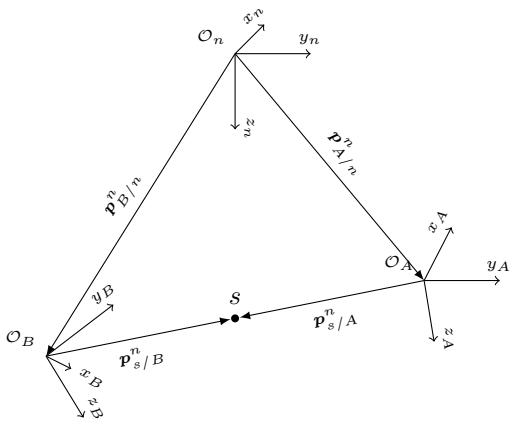

Fig. 2. Constraint vector loop, $\mathcal{O}_n$ is the origin of the inertial space, $\mathcal{O}_i$ for $i \in \{A, B\}$ the origin of each vehicle

There exists multiple approaches for calculating the constraint forces $\boldsymbol{S}_c$. Given n_c constraints on the form in Eq. (16) that is linear in the accelerations.

$$\boldsymbol{A}\left(\boldsymbol{q}, \boldsymbol{s}\right) \dot{\boldsymbol{s}} = \boldsymbol{b}\left(\boldsymbol{q}, \boldsymbol{s}\right) \tag{16}$$

In Udwadia and Schutte (2012) the problem of finding the constraint force was transformed into an optimisation problem using Gauss's Principle of Least Constraints. In this way, the problem of constraint handling becomes a minimisation problem that can be solved using the Moore-Penrose pseudo-inverse. In the end, the constraint vector $\boldsymbol{S}_c$ can be determined by Eq. (17).

$$\boldsymbol{S}_c = \boldsymbol{M}^{1/2}\Big(\boldsymbol{A}\boldsymbol{M}^{-1/2}\Big)^{+}\left(\boldsymbol{b} - \boldsymbol{A}\dot{\boldsymbol{s}_u}\right) \tag{17}$$

where $(\cdot)^{+}$ represents the Moore-Penrose pseudo-inverse. Finally the constrained accelerations of the system can be identified by insertion into Eq. (15) and solving for $\boldsymbol{s}_c$

$$\dot{\boldsymbol{s}}_c = \dot{\boldsymbol{s}}_u + \boldsymbol{M}^{-1/2}\Big(\boldsymbol{A}\boldsymbol{M}^{-1/2}\Big)^{+}\left(\boldsymbol{b} - \boldsymbol{A}\dot{\boldsymbol{s}}_u\right) \tag{18}$$

It is clear from Eq. (18) that Udwadia-Kalaba is a global method as opposed to most impulse based methods.

In many robotic applications quasi-velocities are advantageous compared to generalised velocities. In Klausen et al. (2014) the Udwadia-Kalaba formulation was used to model a system of N multi-copters for the purpose of slung-load transportation using local coordinates.

5. RIGID CONSTRAINT

A main challenge with rigid connected vehicles is that the constraint, which is needed to describe the connection, is restricting all six DOF. This section derives the generic formulation of such rigid constraint. Each of two connected vehicles will have a local body-fixed frame, denoted $\{A\}$ and $\{B\}$, respectively. The rigid constraint is divided into two parts. The first part retains a relative distance between each vehicle to a common point s in the inertial frame. This permits a formulation for a vector loop-closure as shown in Fig. 2.

The second part retains a relative orientation between the vehicles. For quaternions, this relative orientation is the Hamilton product $\otimes$ between the orientation of vehicle A and vehicle B. The constraints are summarised as follows

$$\boldsymbol{c}_1 \;:\; \boldsymbol{p}^n_{A/n} + \boldsymbol{p}^n_{s/A} - \boldsymbol{p}^n_{B/n} - \boldsymbol{p}^n_{s/B} = 0 \tag{19}$$

$$\boldsymbol{c}_2 \;:\; \boldsymbol{u}_A \otimes \boldsymbol{u}^*_B = \boldsymbol{u}_{rel} \tag{20}$$

where $\boldsymbol{u}_A$ is the unit quaternion of vehicle A and $\boldsymbol{u}^*_B$ is the quaternion conjugate of vehicle B.

The second-order time-differentiation of the constraints are required to be brought on the form of Eq. (16). Conducting the time-differentiation on Eq. (19) and recalling that $\dot{\boldsymbol{R}}^n_b = \boldsymbol{S}(\boldsymbol{\omega}^n_{b/n})\boldsymbol{R}^n_b$ yields

$$\dot{\boldsymbol{p}}^n_{A/n} = \boldsymbol{R}^n_A \boldsymbol{\nu}^{(A)}_r \tag{21}$$

$$\dot{\boldsymbol{p}}^n_{s/A} = \boldsymbol{\omega}^n_{A/n} \times \boldsymbol{p}^n_{s/A} \tag{22}$$

The time-differentiation of the expressions (21) and (22) yields

$$\ddot{\boldsymbol{p}}^n_{A/n} = \boldsymbol{R}^n_A \dot{\boldsymbol{\nu}}^{(A)}_r + \boldsymbol{\omega}^n_{A/n} \times \boldsymbol{R}^n_A \boldsymbol{\nu}^{(A)}_r \tag{23}$$

$$\ddot{\boldsymbol{p}}^n_{s/A} = \boldsymbol{\omega}^n_{A/n} \times \boldsymbol{p}^n_{s/A} + \boldsymbol{\omega}^n_{A/n} \times \left(\boldsymbol{\omega}^n_{A/n} \times \boldsymbol{p}^n_{s/A}\right) \tag{24}$$

The derivations of the constraints for vehicle B yields equal result as that of vehicle A with opposite sign. Combining the resulting expression for the constraint matrix $\boldsymbol{A}$ for constraint $\boldsymbol{c}_1$ yields

$$\boldsymbol{A}_1 = \begin{bmatrix} \boldsymbol{R}^n_A & -\boldsymbol{S}(\boldsymbol{p}^n_{s/A}) & -\boldsymbol{R}^n_B & \boldsymbol{S}(\boldsymbol{p}^n_{s/B}) \end{bmatrix} \tag{25}$$

The remaining terms of the expression is included in the constraint vector $\boldsymbol{b}$ which then becomes

$$\begin{aligned} \boldsymbol{b}_1 = &-\boldsymbol{\omega}^n_{A/n} \times (\boldsymbol{R}^n_A \boldsymbol{\nu}^{(A)}_r + \boldsymbol{\omega}^n_{A/n} \times \boldsymbol{p}^n_{s/A}) \\ &+ \boldsymbol{\omega}^n_{B/n} \times (\boldsymbol{R}^n_B \boldsymbol{\nu}^{(B)}_r + \boldsymbol{\omega}^n_{B/n} \times \boldsymbol{p}^n_{s/B}) \end{aligned} \tag{26}$$

For constraint $\boldsymbol{c}_2$ the Hamilton product between the unit quaternion of A and the conjugate of the unit quaternion of B yields the relative rotation between the vehicles. The time-differentiation of the attitude constraint yields

$$\dot{\boldsymbol{u}}_A \otimes \boldsymbol{u}^*_B + \boldsymbol{u}_A \otimes \dot{\boldsymbol{u}}^*_B = \boldsymbol{0} \tag{27}$$

Performing the second time-differentiation of the constraint along with a reduction yields

$$\ddot{\boldsymbol{u}}_A \otimes \boldsymbol{u}^*_B + \boldsymbol{u}_A \otimes \ddot{\boldsymbol{u}}^*_B + 2\left(\dot{\boldsymbol{u}}_A \otimes \dot{\boldsymbol{u}}^*_B\right) = \boldsymbol{0} \tag{28}$$

Transforming this expression into requires additional terms from the change of frame

$$\ddot{\boldsymbol{u}} = \boldsymbol{T}_u \dot{\boldsymbol{\omega}}^b_{b/n} + \dot{\boldsymbol{T}}_u \boldsymbol{\omega}^b_{b/n} \tag{29}$$

To simplify notation an additional matrix is defined below

$$\bar{\boldsymbol{H}}_i = \left[-\boldsymbol{\varepsilon}_i \;\; \eta_i \boldsymbol{I}_3 + \boldsymbol{S}\left(\boldsymbol{\varepsilon}_i\right)\right] \text{ for } i \in \{A, B\} \tag{30}$$

The sign change of the skew-symmetric matrix in $\bar{\boldsymbol{H}}$ compared to $\boldsymbol{H}$ of Eq. (5) results in a change of reference frame from body $\{b\}$ to $\{n\}$ as shown below

$$\boldsymbol{\omega}^b_{b/n} = 2\boldsymbol{H}\dot{\boldsymbol{u}} \tag{31}$$

$$\boldsymbol{\omega}^n_{b/n} = 2\bar{\boldsymbol{H}}\dot{\boldsymbol{u}} \tag{32}$$

The relative quaternion rotation can be expressed in matrix form, linear in either quaternion as follows

$$\begin{aligned} \boldsymbol{u}_A \otimes \boldsymbol{u}^*_B &= \begin{bmatrix} \left(\boldsymbol{u}_B\right)^T \\ \bar{\boldsymbol{H}}_B \end{bmatrix} \boldsymbol{u}_A = \boldsymbol{G}_B \boldsymbol{u}_A \\ &= \begin{bmatrix} \left(\boldsymbol{u}_A\right)^T \\ -\bar{\boldsymbol{H}}_A \end{bmatrix} \boldsymbol{u}_B = \boldsymbol{G}_A \boldsymbol{u}_B \end{aligned} \tag{33}$$

Expanding each term of Eq. (28) combined with Eq. (29) yields

$$2\left(\dot{\boldsymbol{u}}_A \otimes \dot{\boldsymbol{u}}_B^*\right) = 2\begin{bmatrix}\left(\boldsymbol{T}_B\boldsymbol{\omega}_{B/n}^B\right)^T \\ \dot{\boldsymbol{H}}_B\end{bmatrix}\boldsymbol{T}_A\boldsymbol{\omega}_{A/n}^A$$
$$= 2\dot{\boldsymbol{G}}_B\boldsymbol{T}_A\boldsymbol{\omega}_{A/n}^A \tag{34}$$

Each of the terms introducing the quaternion acceleration are brought on linear form as shown below

$$\ddot{\boldsymbol{u}}_A \otimes \boldsymbol{u}_B^* = \boldsymbol{G}_B\boldsymbol{T}_A\dot{\boldsymbol{\omega}}_{A/n}^A + \boldsymbol{G}_B\dot{\boldsymbol{T}}_A\boldsymbol{\omega}_{A/n}^A \tag{35}$$
$$\boldsymbol{u}_A \otimes \ddot{\boldsymbol{u}}_B^* = \boldsymbol{G}_A\boldsymbol{T}_B\dot{\boldsymbol{\omega}}_{B/n}^B + \boldsymbol{G}_A\dot{\boldsymbol{T}}_B\boldsymbol{\omega}_{B/n}^B \tag{36}$$

Finally, the $\boldsymbol{A}$ matrix and $\boldsymbol{b}$ vector for constraint $\boldsymbol{c}_2$ can be displayed as follows

$$\boldsymbol{A}_2 = [\boldsymbol{0}_{4\times3}\ \boldsymbol{G}_B\boldsymbol{T}_A\ \boldsymbol{0}_{4\times3}\ \boldsymbol{G}_A\boldsymbol{T}_B] \in \mathbb{R}^{4\times12} \tag{37}$$
$$\boldsymbol{b}_2 = -\boldsymbol{G}_A\dot{\boldsymbol{T}}_B\boldsymbol{\omega}_{B/n}^B - \left(\boldsymbol{G}_B\dot{\boldsymbol{T}}_A + 2\dot{\boldsymbol{G}}_B\boldsymbol{T}_A\right)\boldsymbol{\omega}_{A/n}^A \tag{38}$$

This concludes the development of the rigid constraint and leads to the model verification of the approach.

6. SIMULATION

6.1 Cases

Two main simulations are conducted to verify the constraint handling and the overall model validity.

Table 1. Initial conditions and thrust output for each vehicle in each simulation

Cases	Initial States	Thrust
Case A	$\boldsymbol{\eta}^{(A)} = [0,0,0,1,0,0,0]$	$\boldsymbol{\tau}^{(A)} = [0,0,0,0,0,0]$
	$\boldsymbol{\eta}^{(B)} = [0,l,0,0.707,0.707,0,0]$	$\boldsymbol{\tau}^{(B)} = [0,0,0,0,0,0]$
Case B	$\boldsymbol{\eta}^{(A)} = [0,0,0,1,0,0,0]$	$\boldsymbol{\tau}^{(A)} = [1,0,0,0,0,0]$
	$\boldsymbol{\eta}^{(B)} = [0,1,0,1,0,0,0]$	$\boldsymbol{\tau}^{(B)} = [1,0,0,0,0,0]$

Two cases 3a and 3b are considered, which are shown in Figure 3.

Case A: Hydrostatic Tests
Case A simulates two vehicles A and B connected by a mass-less rod of length l with relative attitude of 90° in roll. The mass of each vehicle is 20kg, the buoyancy point $\boldsymbol{r}_b^b = [0,0,-0.1]$ in each vehicles local frame and both vehicles are neutrally buoyant. The initial attitude of vehicle B is set to 90° roll. Hence the initial attitude of vehicle A is 0° roll. The purpose of the simulation is to test the interaction between the vehicles exposed to different restoring forces. This simulation is repeated three times, where each iteration changes the length l between the vehicles such that $l \in \{1,2,3\}$.

Case B: Hydrodynamic Tests
Case B simulates two vehicles A and B connected by a mass-less rod of length 1 with zero relative attitude. Both vehicles exerts force in positive surge direction x_b of each vehicle. As with Case A the simulation is conducted three times with increasing surge damping X_u of vehicle B. The purpose of the simulation is to test the interaction between the vehicles when changes occur in the damping. The surge damping of vehicle B is chosen as $X_u \in \{5,10,15\}$.

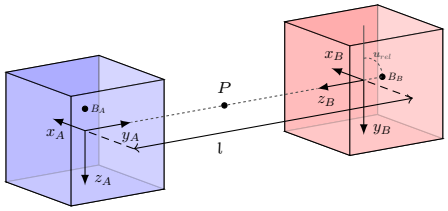

(a) Hydrostatic Test Configuration: Vehicle B is rotated relative to vehicle A such that axis y_A and z_B coincide.

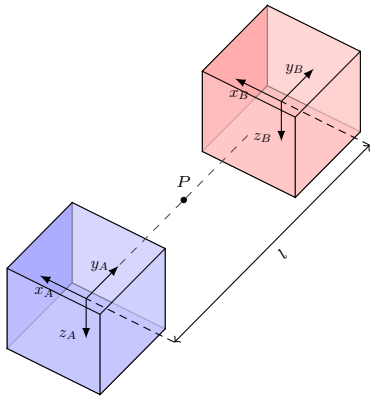

(b) Hydrodynamic Test Configuration: The attitude of both vehicles are identical such that axis y_A and y_B coincide.

Fig. 3. Two configurations containing two vehicles denoted A and B. In both configurations vehicle A is colored blue and vehicle B is colored red.

6.2 Numerical Considerations

Numerical errors in integration procedures cause drift of the constrains. This has profound impact on both the force compensated constraints, but also on the unit constraint in the quaternion.
Constraint drift is a recognised problem in the literature. Braun and Goldfarb (2009) investigated methods for constraint drift removal in the Udwadia-Kalaba equations. The unity constraint on the quaternions can be imposed continuously from the following equation given in Fossen (2011).

$$\dot{\boldsymbol{u}} = \boldsymbol{T}_u\left(\boldsymbol{u}\right)\boldsymbol{\omega}_{b/n}^b + \frac{\gamma}{2}\left(1 - \boldsymbol{u}^T\boldsymbol{u}\right)\boldsymbol{u} \text{ for } \gamma \geq 0 \tag{39}$$

In this paper the Dormand-Prince scheme for integration is used with low tolerance and thereby the error build-up is mitigated.

6.3 Results & Discussion

Case A: Hydrostatic Tests
The simulations of Case A are conducted and the results are shown in Fig. 4 and Fig. 5.

In Fig. 4 the roll angle of both vehicle A and B are shown for each length $l \in \{1,2,3\}$. The relative angular displacement between the vehicles are 90° in relative roll. Since the dynamic profile of the vehicles are identical, the restoring forces will exert an equal and opposite torque on each vehicle when the roll angles are equal and opposite. In the specific case, this angle is $\phi_A = -45°$ and $\phi_B = 45°$. Further, as the length between the vehicles increases so does the period of the roll oscillations. To evaluate the accuracy of the simulation, the results

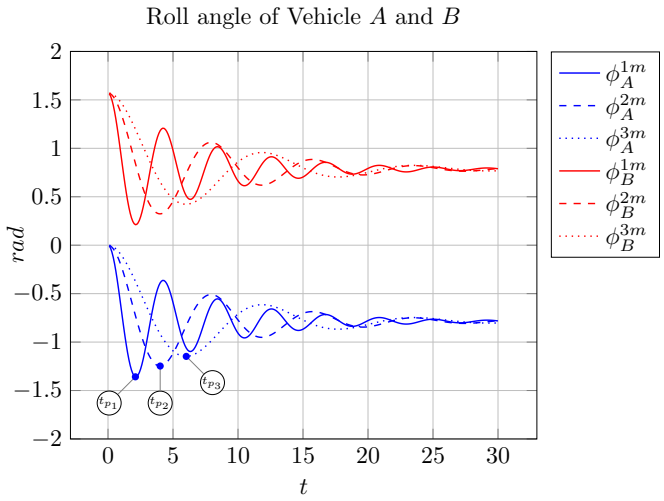

Fig. 4. Roll angle of vehicles A and B for three different rod lengths l. Peak times for vehicle A are marked and coincide with those of vehicle B.

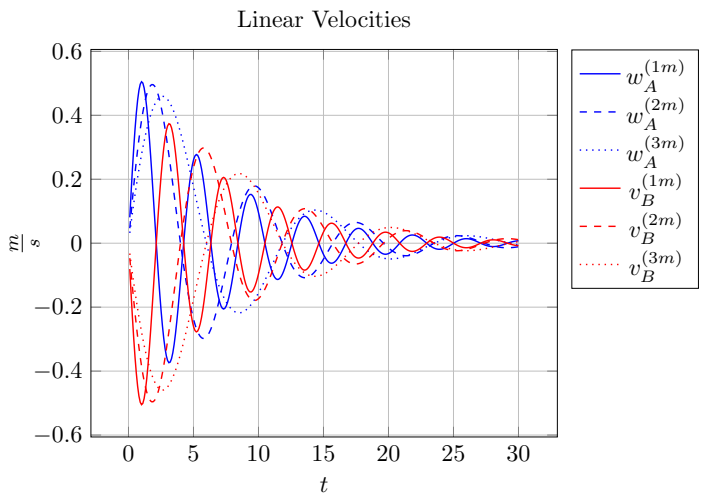

Fig. 5. Heave w of vehicle A and sway v of vehicle B for each simulation at different rod lengths l.

are compared to a simplified analytical solution. The analytical solution is constructed by transforming the two vehicles into a combined system. The inertia of each vehicle is transformed into the centre of mass P of Fig. 3a. The combined buoyancy point is then calculated such that the restoring force of the combined system can be calculated.

Table 2. Comparison of peak times between analytical approximation and simulation.

Peak Time	t_{p_1}	t_{p_2}	t_{p_3}
Analytical	2.07s	3.874 s	5.733s
Simulation	2.107 s	4.013 s	6.02s

The results of the analytical investigation is compared to the simulations in Table 2. Since the roll rate is largely dependent on the inertia of the system, the Huygens-Steiner theorem provides the majority of the contribution to the roll period increase. The deviation of the peak time is attributed to the linearisation of the restoring force vector. This is reasonable since the roll angle of each vehicle depends on the positions and as the distance between them increases they must move further to change the roll angle.

Fig. 5 shows the linear velocity in heave for vehicle A and sway for vehicle B. The results agree with the roll angle since the positive initial roll angle of vehicle B results in a negative torque which acts through the lever arm on vehicle A. In the end vehicle A is forced down in positive heave (z_A) direction while vehicle B will move in negative sway (y_B) direction.

Case B: Hydrodynamic Tests

To verify the hydrodynamic behaviour of the constrained system another simulation is conducted. Here two vehicles are connected by their local sway-axis, such that the relative attitude is zero. This is shown in Fig 3b. The distance between them are fixed at one meter, such that vehicle B is right of vehicle A. Three open-loop simulations are conducted with variation in the hydrodynamic surge coefficient X_u. First a baseline simulation is conducted, where the dynamic profile of the vehicles are identical.

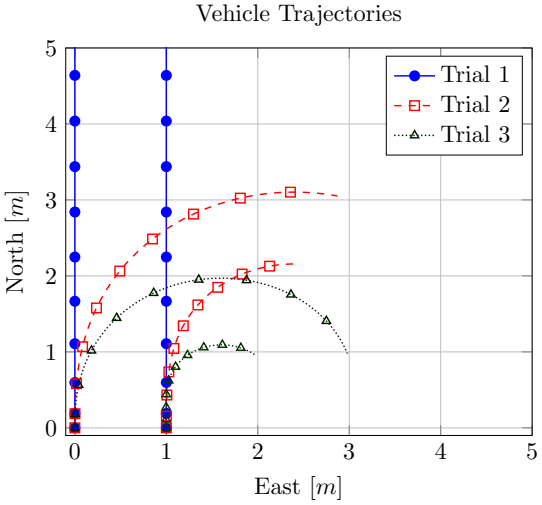

Fig. 6. Three trajectories of open-loop simulations with varying surge damping of vehicle B.

The resulting trajectory is shown as case one in Fig. 6. The centre of mass of the connected systems is right between the vehicles denoted with P in Fig. 3b. Given that the hydrodynamic behaviour is identical, both vehicles will act on the centre of mass with equal and opposite torque and hence the sum of torques are zero. The results is a straight trajectory.

Doubling the surge damping X_u of vehicle B and conducting another simulation yields the results of Fig. 6 Trial 2. Evidently the trajectory is dragged eastwards. The increased surge damping of vehicle B, which is the east positioned vehicle, induces a higher yaw torque on the centre of mass and as expected the trajectory drags eastwards.

Finally the surge damping of vehicle B is further increased to thrice the initial value and the simulation is conducted again. As is expected from previous argumentation, the eastward turn is increased even further.

7. CONCLUSION

This paper has presented an application of a modelling methodology for efficiently describing a system of modular reconfigurable underwater robots. The modelling approach by Udwadia-Kalaba was adopted because it is robust when redundant constraints arise, as is the case for underwater reconfigurable robots, and the approach was shown to maintain the sparsity in the model description and thus make the resulting model feasible for control design and analysis.

A rigid constraint was developed using quasi-accelerations such that the forces acting on each body in the system were applied in local frames. We formulated a combined model of a system of N rigidly connected reconfigurable underwater robots using the Udwadia-Kalaba Equation. To allow the robots to connect in any relative attitude with respect to each other, the attitude representation used was the Euler parameters.

The model was verified using two simulations cases. One considered hydrostatic behaviour between two robots connected by a rod with variable length, a second considered the hydrodynamic behaviour of two connected robots with different properties. Results compared favorably with analytical solutions and physical intuition.

The method is believed to be sufficiently robust to allow for unsupervised automated modelling of connected underwater vehicles.

REFERENCES

Antonelli, G. (2014). *Underwater Robots*, volume 2 of *Springer Tracts in Advanced Robotics*. Springer Berlin Heidelberg, Berlin, Heidelberg. doi:10.1007/978-3-662-14387-2.

Bauchau, O.A. and Laulusa, A. (2008). Review of contemporary approaches for constraint enforcement in multibody systems. *Journal of Computational and Nonlinear Dynamics*, 3(1), 011005. doi:10.1115/1.2803258.

Belleter, D. and Pettersen, K. (2014). Path following for formations of underactuated marine vessels under influence of constant ocean currents. In *53rd IEEE Conference on Decision and Control*, 4521–4528. IEEE. doi:10.1109/CDC.2014.7040095.

Belleter, D. and Pettersen, K. (2015). Underactuated leader-follower synchronisation for multi-agent systems with rejection of unknown disturbances. In *2015 American Control Conference (ACC)*, volume 2015-July, 3094–3100. IEEE. doi:10.1109/ACC.2015.7171808.

Braun, D.J. and Goldfarb, M. (2009). Eliminating constraint drift in the numerical simulation of constrained dynamical systems. *Computer Methods in Applied Mechanics and Engineering*, 198(37-40), 3151–3160. doi:10.1016/j.cma.2009.05.013.

Brenan, K.E., Campbell, S.L., and Petzold, L.R. (1995). *Numerical Solution of Initial-Value Problems in Differential-Algebraic Equations*. Society for Industrial and Applied Mathematics. doi:10.1137/1.9781611971224.

Fossen, T.I. (2011). *Handbook of Marine Craft Hydrodynamics and Motion Control*. Wiley and son, Trondheim, 1st edition.

Gear, C.W. and Petzold, L.R. (1984). ODE Methods for the Solution of Differential/Algebraic Systems. *SIAM Journal on Numerical Analysis*, 21(4), 716–728. doi:10.1137/0721048.

Henriksen, E.H., Berge Gjersvik, T., and Thorkildsen, B. (2015). Positioning of subsea modules using an automated ROV. In *OCEANS 2015 - Genova*, 1–8. IEEE. doi:10.1109/OCEANS-Genova.2015.7271545.

Kalaba, R.E. and Udwadia, F.E. (1994). Lagrangian mechanics, Gauss's principle, quadratic programming, and generalized inverses: new equations for nonholonomically constrained discrete mechanical systems. *Quarterly of Applied Mathematics*, 52(2), 229–241.

Klausen, K., Fossen, T.I., and Johansen, T.A. (2014). Suspended load motion control using multicopters. In *22nd Mediterranean Conference on Control and Automation*, 1371–1376. IEEE. doi:10.1109/MED.2014.6961567.

Mintchev, S., Ranzani, R., Fabiani, F., and Stefanini, C. (2014). Towards docking for small scale underwater robots. *Autonomous Robots*. doi:10.1007/s10514-014-9410-3.

Mintchev, S., Stefanini, C., Girin, A., Marrazza, S., Orofino, S., Lebastard, V., Manfredi, L., Dario, P., and Boyer, F. (2012). An underwater reconfigurable robot with bioinspired electric sense. In *2012 IEEE International Conference on Robotics and Automation*, 1149–1154. IEEE. doi:10.1109/ICRA.2012.6224956.

Takamatsu, M. and Iwata, S. (2008). Index reduction for differential-algebraic equations by substitution method. *Linear Algebra and Its Applications*, 429(8-9), 2268–2277. doi:10.1016/j.laa.2008.06.025.

Udwadia, F.E. and Phohomsiri, P. (2007). Explicit Poincaré equations of motion for general constrained systems. Part I. Analytical results. *Proceedings of the Royal Society A: Mathematical, Physical and Engineering Sciences*, 463(2082), 1421–1434. doi:10.1098/rspa.2007.1825.

Udwadia, F.E. and Schutte, A.D. (2012). A unified approach to rigid body rotational dynamics and control. *Proceedings of the Royal Society A: Mathematical, Physical and Engineering Science*, 468(2138), 395–414. doi:10.1098/rspa.2011.0233.

Vasilescu, I., Kotay, K., Rus, D., Dunbabin, M., and Corke, P. (2005). Data Collection, Storage, and Retrieval with an Underwater Sensor Network. *SenSys*, 154–165. doi:10.1145/1098918.1098936.

Wojtyra, M. and Fraczek, J. (2013). Solvability of reactions in rigid multibody systems with redundant nonholonomic constraints. *Multibody System Dynamics*, 30(2), 153–171. doi:10.1007/s11044-013-9352-0.